

Delimiting the urban growth boundaries with a modified ant colony optimization model



Shifa Ma^{a,b}, Xia Li^{b,*}, Yumei Cai^c

^a Land and Resources Technology Center of Guangdong Province, Guangzhou 510075, Guangdong, China

^b School of Geography and Planning, Guangdong Key Laboratory for Urbanization and Geo-simulation, Sun Yat-Sen University, Guangzhou 510275, Guangdong, China

^c China Land Surveying and Planning Institute, Beijing 100035, China

ARTICLE INFO

Article history:

Received 8 December 2015

Received in revised form 5 November 2016

Accepted 11 November 2016

Available online xxxxx

Keywords:

Urban growth boundary

Land use planning

Ant colony

Spatial optimization

Urban agglomeration

ABSTRACT

Delimiting urban growth boundaries (UGBs) has been generally regarded as a regulatory measure for controlling chaotic urban expansion. There are increasing demands for delimiting urban growth boundaries in fast growing regions in China. However, existing methods for delimiting UGBs mainly focus on intrinsic dynamic processes of urban growth and ignore external planning interventions. Delimiting UGBs to restrain chaotic expansion and conserve ecological areas is actually a spatial optimization problem. This study aims to develop an optimization-based framework for delimiting optimal UGBs by incorporating dynamic processes and planning interventions into an ant colony optimization (ACO) algorithm. Local connectivity, total utility values and quantity assignment were integrated into the exchange mechanism to make ACO adaptive for the delimitation of UGBs. The core area of Changsha-Zhuzhou-Xiangtan urban agglomeration, a very fast growing area in Central China was selected as the case study area to validate the proposed model. UGBs under multi planning scenarios with given combinations of weights for urban suitability, high-quality farmland protection, and landscape compactness were efficiently derived from the ACO model. Hypothetic datasets were initially used to test the performance of ACO on global optimum and its ability to optimize complex landscape patterns. Compared with experts' planning scenario, the optimal UGBs delimited by ACO model is practical. Results indicate that spatial optimization methods are plausible for delimiting optimal UGBs.

© 2016 Elsevier Ltd. All rights reserved.

1. Introduction

A large amount of non-urban land has been converted into urban land with the development of economy and society, and this trend is observable in fast urbanizing regions (Lambin & Meyfroidt, 2011). In China, urbanization levels rose dramatically in the past 30 years and have currently reached over 50%. However, most cities have shown pell-mell expansion patterns, which would cause a series of ecological and environmental problems, such as farmland erosion, forest degradation, and among others (Hoekstra & Wiedmann, 2014; Wei & Ye, 2014). In this case, it is an urgent problem to design a suitable spatial pattern for directing urban growth.

It has proven that smart urban growth can increase the density of urban services and protect surrounding natural ecosystems (Jun, 2004). The scope and pattern of urban-land allocation must initially be restrained in a certain areas, and the edge of it can be actually defined

as the urban growth boundaries (UGBs) (Nelson & Moore, 1993). Establishing UGBs has been regarded as a regulatory measure for directing smart urban growth (Knaap & Hopkins, 2001). UGBs can be traced back to the concept of Great Britain's green belt in 1930s, but they were really used as an urban planning tool about in 1960s. In the United States, the typical UGBs were established in 1958 around Lexington, Kentucky, and particularly UGBs carried forward by Portland, Oregon has been taken as a classical reference for other cities (Nelson & Moore, 1993). Currently, UGBs have played an important role and become a cultural symbol in urban planning (Abbott & Margheim, 2008). America has taken UGBs as a significant tool to direct the smart growth and made them of legal qualification (Hepinstall, Coe, & Hutyr, 2013; Knaap & Hopkins, 2001). Many other countries such as Swiss and India have also managed to promote the efficiency of UGBs on urban planning. In China, delineation of UGBs has been given significant attention by government and researchers in recent years. Some big cities have been aware that it is important to delimit UGBs for restraining the pell-mell urban growth, and different similar policy such as basic ecological line in Shenzhen has been correspondingly put forward. A total of 14 cities such as Beijing, Shanghai, Guangzhou, Xiamen, and among others were selected as piloting areas to delimit UGBs in 2014, and this task was expected to be finished in 2015. Some

* Corresponding author at: School of Geography and Planning, Guangdong Key Laboratory for Urbanization and Geo-simulation, Sun Yat-sen University, 135 West Xingang RD., Guangzhou 510275, China.

E-mail addresses: whuma@163.com (S. Ma), lixia@mail.sysu.edu.cn (X. Li), caiyumei@263.net (Y. Cai).

researchers have also selected Beijing and Jinan as case study areas to discuss the implementation procedure of UGBs delineation (Gennaio, Hersperger, & Bürgi, 2009; Long, Han, Lai, & Mao, 2013; Venkataraman, 2014; Zheng & Lv, 2016). The application of UGBs as a significant tool to direct the smart growth is being carried forward by Chinese government.

The increasing popularity of UGBs for restraining pell-mell expansion requires efficient and feasible techniques to delimit those boundaries especially in China. A large number of methods have been applied in solving this problem. For example, UGBs could be delineated by planners with experiences. However, UGBs delimited by planners' artworks lack of quantitative analysis and the patterns delimited by different experts may show great difference (Long et al., 2013). Therefore, models have been developed to identify the probable boundaries quantitatively. Land use suitability evaluation models have been widely used to delimit UGBs (Bhatta, 2009). In those models, urban land use suitability is commonly evaluated from a series of spatial factors, e.g. topography and traffic conditions (Cerreta & De Toro, 2012). Although these evaluation methods are easy to implement, it is difficult to estimate the contribution of geographical factors to potential urban suitability in future (Kiran & Joshi, 2013). Moreover, in the view of urban-land allocation, not only suitability but also landscape patterns are the significant aspects (Cao, Huang, Wang, & Lin, 2012). Landscape characteristics are commonly ignored when delineating UGBs if only suitability evaluation models were considered (Santé, Crecente, & Miranda, 2008a).

As is well known, cities are dynamic systems influenced by both anthropogenic activities and natural processes (Washington-Ottombre et al., 2010). Urban growth pattern can be predicted from spatio-temporal variation trends of urban dynamics. Data mining algorithms such as spatial logistic regression (SLR) and artificial neural network (ANN) have been adopted to discover the urban growth probability (Tayyebi, Perry, & Tayyebi, 2014; Tayyebi, Pijanowski, & Tayyebi, 2011). Compared with land use suitability models, these models can identify the contribution of spatial driving factors from the selected training samples, but they generally ignore the local interaction among land use cells (Batty & Xie, 1999). Bottom-up based geo-simulation models such as cellular automata (CA), which integrate the spatial growth probability and local interaction, have been then applied to the prediction of land conversion in future (Li, 2011; Santé, García, Miranda, & Crecente, 2010). UGBs can thus be delimited from the simulation result of urban expansion (Long et al., 2013; Mitsova, Shuster, & Wang, 2011).

However, future urban growth does not strictly follow historical rules. For example, the government may regulate the growth direction in terms of socio-economic status and some special planning objectives such as ecological conservation (Long, Gu, & Han, 2012), and thus, the delimitation and prediction of UGBs based on historical rules is not always reasonable. Planning regulation and planning demands should be involved for the delineation of UGBs. Therefore, the balance among urban growth processes, planning regulations, and landscape characteristics appeals to the attention of UGBs delimitation (Gordon, Simondson, White, Moilanen, & Bekessy, 2009), which can be viewed as a land use spatial optimization problem (Ligmann-Zielinska, Church, & Jankowski, 2008). Simple GIS spatial analysis tools and process-based simulation models cannot obtain optimal results (Li, Chen, Liu, Li, & He, 2010). It is, therefore, essential to introduce spatial optimization models for delimiting UGBs.

Although UGBs are just designed as boundary lines, they can essentially be viewed as optimal patterns of urban-land allocation in the future. According to current researches, genetic algorithms (GA) (Brookes, 2001), simulated annealing (SA) (Santé, Boullón, Crecente, & Miranda, 2008b), particle swarm optimization (PSO) models (Liu, Wang, Ji, Liu, & Zhao, 2012a; Masoomi, Mesgari, & Hamrah, 2013), ant colony optimization (ACO) algorithms (Li, Lao, Liu, & Chen, 2011), etc. have proven to be effective in solving such land use optimization problem. In those models, ACO has proven to be the most efficient in solving area optimization problems such as zoning protected natural areas and

multi-type land use allocation, which are involved with conflicts among multiple objectives, implemented on raster surfaces (Li et al., 2011; Liu, Li, Shi, Huang, & Liu, 2012b). Therefore, this study aims to develop an optimization-based framework in which a modified ACO has been devised for creating optimal UGBs, and a fast growing area of Changsha-Zhuzhou-Xiangtan urban agglomeration in Central China is selected as the case study area to validate the availability of the proposed model.

2. Problem statement and methodology

2.1. Defining the mathematical model for delimiting UGBs

The essence of UGBs delineation is to constrain urban growth within a given region, protect surrounding rural landscapes and explore optimized urban spatial patterns in the geo-space (Cho, Chen, Yen, & Eastwood, 2006), which can be expressed as the set of grid cells in a two-dimensional matrix with I rows and J columns. The land inside the UGBs is allowed for urban growth, whereas the land outside the UGBs is set aside for farming, forestry, and low-density residential development (Abbott & Margheim, 2008). Optimal UGBs are to assign urban land for the most probably connected cells, which is aim to balance the conflicts between urban growth and ecological conservation. The status of a cell in row i ($i = 1, 2, \dots, I$) and column j ($j = 1, 2, \dots, J$) can be represented as a binary variable x_{ij} and $x_{ij} \in \{0, 1\}$, such that $x_{ij} = 1$ if the cell is allowed for urban growth; otherwise, $x_{ij} = 0$. Whether cell (i, j) is 1 or 0 is determined by the given objectives and constraints. Then, the urban growth boundaries can be derived from the edge of the patches labeled as 1. In this study, the objectives and constraints defined in the model are listed as follows.

2.1.1. Objectives

2.1.1.1. Maximum suitability for urban growth. Urban growth is mainly influenced by a series of spatial factors, and the suitability of a land cell for urban growth is often expressed as the status of location condition (e.g. transportation, topography, and surrounding environment) (Kiran & Joshi, 2013). Maximum suitability is calculated using the following equation:

$$\text{Max } f_{\text{suitu}} = \frac{\sum_{i=1}^I \sum_{j=1}^J x_{ij} \times \text{Suit}U_{ij}}{\sum_{i=1}^I \sum_{j=1}^J x_{ij}} \quad (1)$$

where f_{suitu} is the average suitability of the growth pattern, $\text{Suit}U_{ij}$ is the suitability of cell (i, j) for allocating urban land.

2.1.1.2. Maximum preservation for high-quality farmlands. Encroaching on a number of farmlands is inevitable for urban growth. However, the immoderate occupation must be restrained for food security (Godfray et al., 2010). The quality of farmlands determines the quantity and location of those preserved, farmlands of the highest quality have the highest probability to be preserved. The value for measuring maximum farmland preservation is calculated as follows:

$$\text{Max } f_{\text{farmp}} = \frac{\sum_{i=1}^I \sum_{j=1}^J x_{ij} \times (1 - \text{Suit}F_{ij})}{\sum_{i=1}^I \sum_{j=1}^J x_{ij}} \quad (2)$$

where f_{farmp} represents the average level of high-quality farmlands preserved. $\text{Suit}F_{ij} \in (0, 1)$ is defined as the quality of farmland, which can be measured using the suitability evaluation of agricultural land use.

2.1.1.3. *Maximum compactness of UGBs pattern.* If only the urban suitability and high-quality farmland preservation are considered for UGBs optimization, then urban land may distribute as fragmentary patterns. Actually, the future state of a cell is also influenced by its neighbor cells, a compact urban patch is preferred by developers to perform development activities (Santé et al., 2008a). The landscape pattern of urban patches is also significant to planning layout. Compactness index has been used to measure the landscape pattern, which is characterized as the ratio of the area to the perimeter for every urban patch (Li et al., 2011). In this study, average compactness index is adopted so as to make urban patches regular and is expressed as:

$$Max f_{compu} = \left(\sum_{p=1}^P \frac{2\pi\sqrt{a_p/\pi}}{l_p} \right) / P \quad (3)$$

where f_{compu} is the average compactness of urban patches, P is the total number of urban patches, a_p and l_p are the area and the perimeter of patch p respectively, $p = 1, 2, \dots, P$.

Based on these conflicting objectives, two popular methods including Pareto selection and the weight combination have been efficiently used to solve this problem (Huang, Fery, Xue, & Wang, 2008; Santé et al., 2008b). In this study, the final objective (utility) function for UGBs delimitation is designed to provide alternative solutions with the use of a weight combination. The expression is given as follows:

$$F_{UGBs} = w_{suitu} \times f_{suitu} + w_{farmp} \times f_{farmp} + w_{compu} \times f_{compu} \quad (w_{suitu} + w_{farmp} + w_{compu} = 1) \quad (4)$$

where F_{UGBs} is the total utility. The parameters of w_{suitu} , w_{farmp} , and w_{compu} are the weights assigned to urban suitability, farmlands preservation, and landscape compactness respectively. Optimal UGBs should achieve the best utility with the given weight combination.

2.1.2. Constraints

When delimiting the UGBs, not all cells can be used for urban growth because of physical attributes and ecological conservation. Meanwhile, the scope of UGBs in a planning period is mainly influenced by socio-economic development. Therefore, quantitative and spatial constraints should be incorporated into UGBs optimization in terms of external planning interventions.

2.1.2.1. *Scope of UGBs.* The scope of UGBs is determined and adjusted according to the socio-economic development in a planning period (He, Okada, Zhang, Shi, & Zhang, 2006). In most cases, annual urban growth rate is adopted to measure the total quantity of urban land in a region, that is, the scope of UGBs, using statistical analysis methods (Lambin & Meyfroidt, 2011). However, subregions such as different administrative districts of the city playing dissimilar roles in future urban growth (Altieri, Cocchi, Pezzi, Scott, & Ventrucci, 2014). The quantities assigned for subregions will influence the internal structure of urban growth in any planning period. Therefore, the quantity of urban land for each subregion should be coordinated and constrained to obtain optimal UGBs. The scope of UGBs can be correspondingly expressed as:

$$\lambda_s \leq \sum_{i=1}^R \sum_{j=1}^C x_{ij} \cdot Z_s \leq \mu_s, \quad \forall s \in S \quad (5)$$

where S is the total number of subregions and Z_s is a binary variable that identifies if cell (i, j) belongs to the s th subregion. If cell (i, j) is contained within the s th subregion, then $Z_{ij} = 1$; otherwise, $Z_{ij} = 0$. Meanwhile, if the cell (i, j) in the s th subregion is allocated with urban land, then $x_{ij} = 1$, otherwise, $x_{ij} = 0$. λ_s and μ_s , which are the minimum and maximum number of cells planned for the s th subregion respectively. This constraint can regulate and balance the quantity assignment of urban land among subregions.

2.1.2.2. *Spatial constraints.* Land use preserved for ecological services must be excluded from urban-land allocation (Reza & Abdullah, 2011). Physical or legal characteristics have been considered as important constraints to prevent a cell from urban expansion (Tayyebi et al., 2011). These constraints generally include elevation, location of mountains, and government-protected lands (e.g., forests, wetlands, basic farmlands, and lakes). Newly increased urban land cannot encroach on cells classified into ecological conservation areas or inappropriate for urban expansion. This can be expressed as follows:

$$x_{ij} \neq 1, \quad \forall cell(i, j) \in C \quad (6)$$

where C is the set of cells forbidden for urban growth.

2.2. Optimizing UGBs with modified ACO

2.2.1. Classical ACO algorithm

With the objectives and constraints described above, ACO is modified to delimit UGBs, that is, obtain the near-optimal solution of Eq. (4). The ACO algorithm, which was first proposed by Italy scholar Dorigo in the 1990s (Dorigo, Maniezzo, & Colorni, 1996), can solve various optimization problems by simulating the behavior of ants in seeking foods. The mechanism of classical ACO can be explained through solving the traveling salesman problem (TSP) which is to find the shortest tour connecting N given cities (Dorigo et al., 1996). In TSP optimization, the probability of an ant selecting a path moving from city u to city v is determined by both pheromone trail and heuristic information. It is expressed as (Dorigo et al., 1996):

$$\hat{p}_{uv}^k(t) = \begin{cases} \frac{[\tau_{uv}(t)]^\alpha \cdot [\eta_{uv}(t)]^\beta}{\sum_{k \in C^k} [\tau_{uk}(t)]^\alpha \cdot [\eta_{uk}(t)]^\beta} & \text{if } v \in C^k \\ 0 & \text{otherwise} \end{cases} \quad (7)$$

where $\hat{p}_{uv}^k(t)$ is the transition probability from city u to city v for the k th ant at time t , $\tau_{uv}(t)$ is the amount of pheromone trail on path (u, v) , and $\eta_{uv}(t)$ is a heuristic function related to visibility (travel distance). The set C^k represents the cities that can be visited again without any repetition. A taboo list is used to prevent an ant from traveling the visited cities again. α and β are used to control the relative importance of the pheromone trail versus the visibility (travel distance).

At each iteration time, the amount of the pheromone trail is updated according to the following equations (Dorigo et al., 1996):

$$\tau_{uv}(t + 1) = (1 - \rho)\tau_{uv}(t) + \Delta\tau_{uv}(t) \quad (8)$$

$$\Delta\tau_{uv}(t) = \sum_{k=1}^K \Delta\tau_{uv}^k(t) \quad (9)$$

where ρ is the evaporation rate of the pheromone trail between time t and $t + 1$, $\Delta\tau_{uv}^k(t)$ is the quantity of the trail substance per length unit laid on path (u, v) by the k th ant between time t and $t + 1$, and K is the number of ants traveling the path (u, v) . $\Delta\tau_{uv}^k(t)$ is calculated with the following equation:

$$\Delta\tau_{uv}^k(t) = \begin{cases} \frac{Q}{L_k} & \text{if ant } k \text{ visited } (u, v) \\ 0 & \text{otherwise} \end{cases} \quad (10)$$

where Q is a constant which can be subjectively defined. In most cases, it is given as the value of 1, and the whole equation represents the accumulated quantity of the trail substance per length unit laid on the traveling path within a time interval in TSP problem (Dorigo et al., 1996). L_k is the tour length or total travel cost of the k th ant.

The heuristic function $\eta_{uv}(t)$ is commonly calculated as the inverse of the distance (d_{uv}) between city u and city v (Dorigo et al., 1996). A

shorter route connecting city u with city v will have higher probability of being selected by an ant.

2.2.2. Modifying ACO for the delineation of UGBs

The delineation of UGBs aims to achieve the global optimized patterns for future urban growth. ACO algorithm should be modified to adapt the designed objectives and constraints. Heuristic function and pheromone trail must be adjusted to delimit the optimal UGBs.

2.2.2.1. Heuristic function. Heuristic function is designed to guide the traveling of ants, which were usually calculated only using the suitability for area optimization problem (Li et al., 2011). However, using suitability alone to calculate heuristic information may cause dispersive urban patches scattered within the UGBs (Bhatta, 2009). During the delineation of plausible UGBs, an artificial ant is inclined to select local connected and compact patches with high urban suitability and superior quantities of high-quality farmlands preserved. The constraint of local connectivity is thus incorporated into the heuristic function and expressed as follows:

$$\eta_{ij}^k(t) = w_{suitu} \times SuitU_{ij} + w_{farmp} \times (1 - SuitF_{ij}) + w_{compu} \times \frac{\sum_{i-\Omega}^{i+\Omega} \sum_{j-\Omega}^{j+\Omega} x_{ij}^k}{(2 * \Omega + 1)^2} \quad (11)$$

$$\Omega = \Omega_{max} - \frac{T_c \times (\Omega_{max} - \Omega_{min})}{T} \quad (12)$$

where $\eta_{ij}^k(t)$ is the heuristic function on cell (i, j) for the k th ant at time t , and w_{suitu} , w_{farmp} , and w_{compu} are the weights for suitability, farmland preservation, and compactness, respectively. The local connectivity is calculated using the urban density within a dynamic neighborhood to group small patches together. Ω represents the neighborhood of cell (i, j) . Ω_{max} and Ω_{min} are maximum and minimum sizes of the neighborhood, respectively. Then the size of connected patches is determined by the size of neighborhood window. Ω_{min} is usually set as the size of a Moore neighborhood, whereas Ω_{max} is a subjective value set with the decision-makers' experience. The larger the value of Ω_{max} is, the larger the connected patch is. In this study, Ω_{max} is assigned with the average size of urban patches in 2015. The neighborhood window Ω is diminished from Ω_{max} to Ω_{min} during the iterative process. T and T_c are the numbers of total iteration times and current iteration time, respectively.

2.2.2.2. Pheromone trail accumulation. During the optimization process, ants can visit any cell available for allocating urban land and release pheromone trail on the visited cells. The amount of deposited pheromone is related to the total utility of the urban allocation pattern. A cell with the larger amount of pheromone can attract ants to select it, and additional more amount of pheromone is deposited on this cell. Pheromone feedback among the artificial ants can correspondingly generate the maximum utility, and the allocation pattern selected by any ant represents a solution. Hence, the global pheromone trail is accumulated using the average utility of a solution and expressed as:

$$\tau_{ij}(t) = (1 - \rho) \times \tau_{ij}(t-1) + \frac{\sum_{k=1}^K x_{ij}^k F_{UGB}^k(t)}{\sum_{k=1}^K x_{ij}^k} \quad (13)$$

where $\tau_{ij}(t)$ and $\tau_{ij}(t-1)$ are the pheromone trail deposited on cell (i, j) by all the ants at time t and time $t-1$, respectively; $F_{UGB}^k(t)$ is the total utility of the urban allocation pattern selected by the k th ant calculated using the Eq. (4) at time t .

2.2.2.3. Probability calculation. The cell (i, j) selected by ant k ($k = 1, 2, \dots, K$) for allocating urban land is finally determined by the transition probability. The conventional expression representing the combination between heuristic information and pheromone trail for area optimization problems is similar with Eq. (7) (Li et al., 2011). The linear expression can be derived from the log transformation of Eq. (7). A modified expression is adopted to calculate the transition probability and is expressed as:

$$\hat{p}_{ij}^k(t) = \begin{cases} \omega \times \tau_{ij}(t) + (1 - \omega) \times \eta_{ij}^k(t) & \text{if } ij \in C \\ 0 & \text{otherwise} \end{cases} \quad (14)$$

where \hat{p}_{ij}^k is the probability for the k th ant to allocate urban land on cell (i, j) , ω is the given weight used to control the relative importance of the pheromone trail versus the heuristic information, and C is the set of cells unavailable for allocating urban land.

2.2.2.4. Status updating and UGBs delineation. At the initial stage, the solution formed by any ant k is randomly generated. The utility $F_{UGB}^k(t)$ under the given weight combination in Eq. (4) is calculated and released to all the cells traveled by ant k . $\tau_{ij}(t)$, $\eta_{ij}^k(t)$, and \hat{p}_{ij}^k are then calculated. The probabilities of all the non-urban cells to be selected by ant k are sorted in descending sequence. The higher the probability is, the non-urban cell will have a more chance to be selected. Accordingly, all the non-urban cells of higher probability are updated with urban land under the quantity constraint calculated using Eq. (5) in each iteration. When the total utility value F_{UGB}^k is inclined to be a stable value during the iterations, the optimal pattern of urban-land allocation formed by ant k can be obtained. Then UGBs can be delimited from the edge of the pattern with the highest utility. If the weight combination is changed, then the pattern of delimited UGBs will correspondingly varied. Fig. 1 illustrates the main procedure of delimiting UGBs using ACO.

3. Model implementation and results discussion

3.1. Study area and materials

The core area of Changsha-Zhuzhou-Xiangtan urban agglomeration (CZTUA) in Central China was selected as the case study area to validate the proposed model. This region contains three municipal centers (Changsha, Zhuzhou and Xiangtan) and 15 county level zones (Fig. 2). The three municipal cities are connected with each other tightly within 40 km along the Xiangjiang River. This region is turning to be the economic growth pole in Hunan province with a total area of 6084 km², a total population of approximately 60 million, and a total GDP of over 1000 billion Yuan RMB in 2015. As a typical urban agglomeration in Central China, CZTUA has undergone rapid urbanization. By the year of 2015, the urbanization level has reached 64%. Regulating the urban growth of CZTUA has turned to be an important strategy for building cities oriented with "resource-saving and environment-friendly". Delineation of UGBs is essential to balancing urban growth and environment conservation in CZTUA.

Remote sensing images and GIS spatial data mainly including DEM, road networks, transportation centers, administration centers, and among others were used to assist UGBs delineation. Landsat images (124-40, 123-41) collected in 2005, 2010, and 2015 were used to retrieve urban land. DEM and Landsat images were downloaded from the United States Geological Survey website. Land use maps were visually interpreted and classified from Landsat images, and the interpretation accuracy is up to approximately 92% with the validation of Google earth images. Other spatial data was obtained from Provincial Geomatic Center of Hunan province. All spatial datasets were converted with the same projection and the resolution.

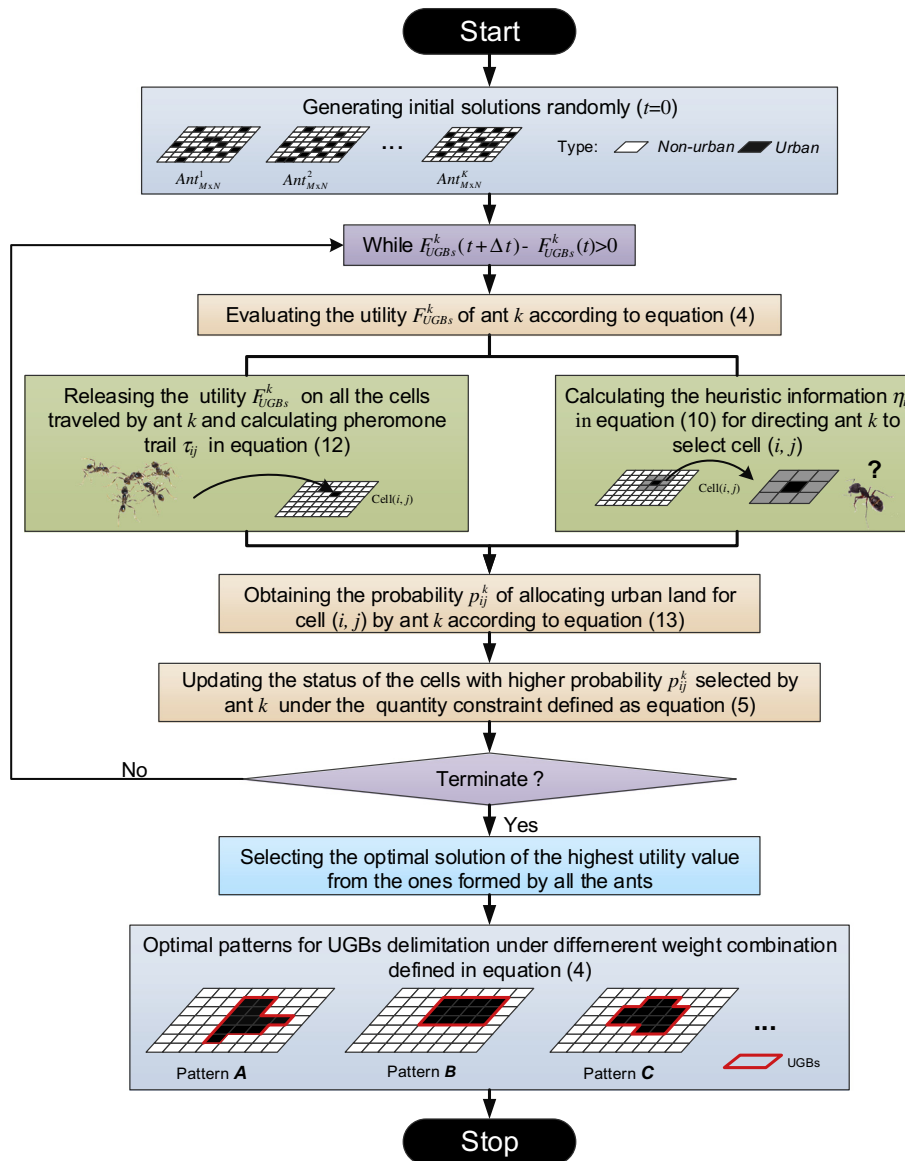


Fig. 1. Flowchart of the ACO model for delimiting UGBs.

3.1.1. Land use suitability evaluation

It has proven that the urban suitability was greatly determined by topographic and traffic conditions (Liu, Wang, et al., 2012). In this study, the urban suitability in Eq. (1) was calculated by using a total of 12 spatial variables including distance to development centers (e.g., municipal centers, provincial capital, county centers, and urban patches), distance to transportation conditions (e.g., county roads, provincial roads, national roads, highways, railway stations, and airports), and topographic conditions (e.g., elevation and slope). Values of all these variables are normalized within the range of 0–1 considering their maximum impact to urban growth. Analytic hierarchy process (AHP), which can effectively support decision making with regard to complex issues that involve the comparison of decision elements (Tudes & Yigiter, 2010), was used to calculate the weights for the selected factors. The pairwise comparison matrix was built based on the contribution of these factors to urban growth, which was analyzed and concluded from the distribution pattern of newly increased urban land during the period 2005–2013. Similarly, we can also calculate the agriculture land suitability in Eq. (2) by using the factors to identify the quality of farmland. The parameters of great soil group, land use

capability class, land use capability sub-class, soil depth, slope, elevation, erosion level and other soil properties were used (Akinci et al., 2013). The consistency ratio of AHP for evaluating urban suitability and agriculture land suitability was 0.0745 and 0.067, respectively, which were less than 0.1. The suitability maps were used as the basic input data for ACO model.

3.1.2. Ecological sensitive areas recognition

Ecological sensitive areas and lands for ecological service should be prevented from urban growth, mainly including rivers, mountains, forest parks, natural conservation areas, and scenic areas (Li et al., 2011). Therefore, Xiangjiang River, Yuelu Mountain, Orange Isle, green belt among three municipal cities, and other large-scale rivers are excluded from urban expansion.

3.1.3. Quantity of urban growth for each subregion

Delineation of UGBs should also consider the growth directions and quantitative balance between subregions. In this study, we used the county level administrative districts as the subregions. It was assumed that urban growth in CZTUA would continue with the same average

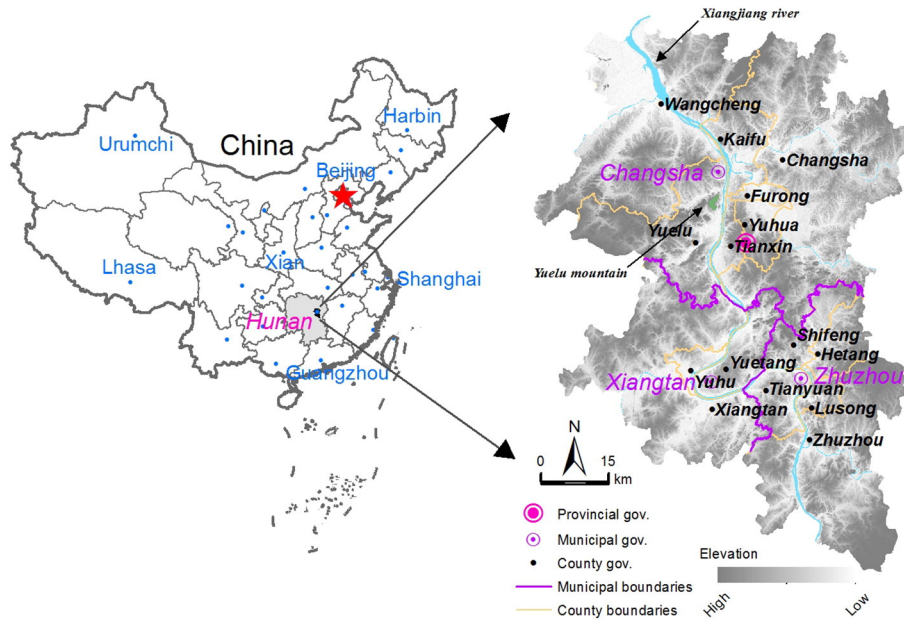


Fig. 2. Location and the core area of Changsha-Zhuzhou-Xiangtan urban agglomeration.

annual rate as that during the period 2000–2015. The quantity of urban land for each subregion in 2030 defined as Eq. (5) was then predicted.

3.2. Results analysis

The three objectives (i.e. maximum suitability for urban growth, maximum preservation for high-quality farmlands, and maximum compactness of UGBs pattern) may conflict with each other, and decision-makers show different preferences for these objectives. The composite optimality score can be defined in different ways by emphasizing different objectives to generate alternative patterns (Santé et al., 2008a; Li et al., 2011; Liu et al., 2012b). The values of the weight for each objective ranging from 0 to 1 can be set, and various combinations can be generated to analyze the sensitivity of the proposed model. The weight for each objective was divided with the interval of 0.25 in this study, and the corresponding weights are 0, 0.25, 0.5, 0.75, and 1. Table 1 shows the feasible weight combinations we have set for the three objectives to generate different UGBs patterns. Options A, C, and F can be eventually viewed as the optimization that tries to maximize both urban suitability and farmland protection. The relative weights of 3:0:1, 1:0:1, and 1:0:3 were given to generate allocation patterns that maximize suitability and compactness of urban land masses (options B, E, and I). The relative weights of 2:1:1, 1:2:1, and 1:1:2 were given to generate

allocation patterns that maximize all the three objectives (options D, G, and H). Fig. 3 shows the corresponding optimization results.

Figs. 3(a), (c), and (f) show that the urban-land allocation patterns under options A, C, and F are fragmented. Newly increased urban lands are mainly located around urbanized areas or are adjacent to roads and are kept away from high-quality farmlands, because the compactness wasn't incorporated into the utility function. When increasing the weight for farmland preservation, the average suitability and total utility value turn to be decreased, the patterns are more fragmented, and a few high-quality farmlands of superior location conditions are excluded from urban growth. Fig. 3(b), (e), and (i) show that the delineation patterns are more compact with the increasing weight for compactness, the utility values also show great difference among the allocation patterns with the various weight combinations for suitability and compactness. However, a few high-quality farmlands are encroached on by urban land without considering ecological conservation. Options D, G, and H are to form the allocation patterns considering the trade-off among suitability, farmland protection and landscape compactness. The increasing weight for farmland preservation results in fragmented patterns, and the increasing weight for compactness results in lower utility values of suitability and farmland preservation. The patterns of UGBs delimited under different weight combinations show that the weight for suitability ranging from 0.50 to 0.75, weight for high-quality farmland preservation ranging from 0 to 0.25, and weight for compactness approximated at 0.25 are rational for application.

Table 1

Optimum values with different multi-objectives integrated.

| Options | Weights | | | f_{suitu} | f_{farmp} | f_{compu} | F_{UGB} |
|------------------|-------------|-------------|-------------|-------------|-------------|-------------|-----------|
| | W_{suitu} | W_{farmp} | W_{compu} | | | | |
| A [Figure 8 (a)] | 0.75 | 0.25 | 0.00 | 0.9606 | 0.6746 | 0.9814 | 0.8891 |
| B [Figure 8 (b)] | 0.75 | 0.00 | 0.25 | 0.9669 | 0.5184 | 0.9963 | 0.9743 |
| C [Figure 8 (c)] | 0.50 | 0.50 | 0.00 | 0.9268 | 0.7403 | 0.9848 | 0.8336 |
| D [Figure 8 (d)] | 0.50 | 0.25 | 0.25 | 0.9572 | 0.6279 | 0.9887 | 0.8828 |
| E [Figure 8 (e)] | 0.50 | 0.00 | 0.50 | 0.9581 | 0.5309 | 0.9756 | 0.9669 |
| F [Figure 8 (f)] | 0.25 | 0.75 | 0.00 | 0.8985 | 0.7643 | 0.9586 | 0.7979 |
| G [Figure 8 (g)] | 0.25 | 0.50 | 0.25 | 0.9112 | 0.7384 | 0.9409 | 0.8322 |
| H [Figure 8 (h)] | 0.25 | 0.25 | 0.50 | 0.9451 | 0.6106 | 0.9695 | 0.8737 |
| I [Figure 8 (i)] | 0.25 | 0.00 | 0.75 | 0.9501 | 0.5354 | 0.9974 | 0.9856 |

3.3. Discussion

3.3.1. Performance of the proposed model on spatial optimization

To validate the performance of the proposed model on UGBs delimitation, we should verify if the model can obtain the global best optimum. The hypothetical data whose optimal pattern is easy to be identified can be used to validate the performance of optimization model (Li et al., 2011; Liu et al., 2012b). In this study, considering the objectives and constraints designed in the ACO model, we used three sets of hypothetical data with the same resolution and size to validate the performance of the ACO model in theory. And the preliminary test is divided into three parts: (1) performance on local and global optimums;

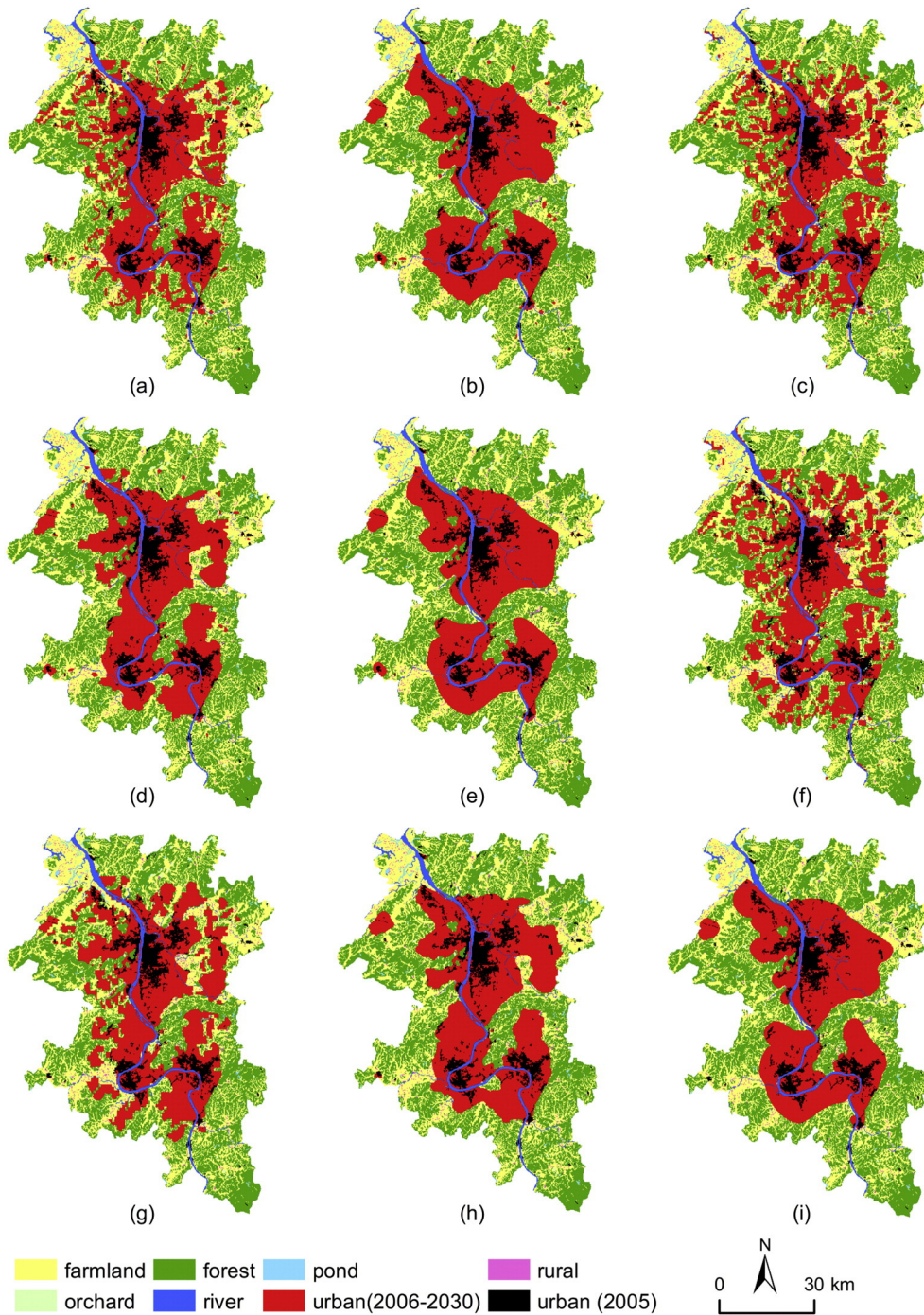


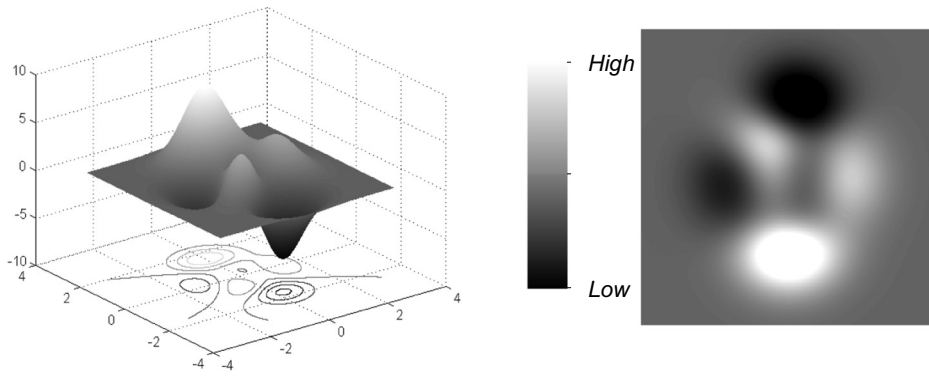
Fig. 3. Urban growth patterns of CZTUA obtained from the ACO model with various weighting scheme options.

(2) ability to obtain connected landscape patterns; and (3) efficiency in optimizing complex spatial structures.

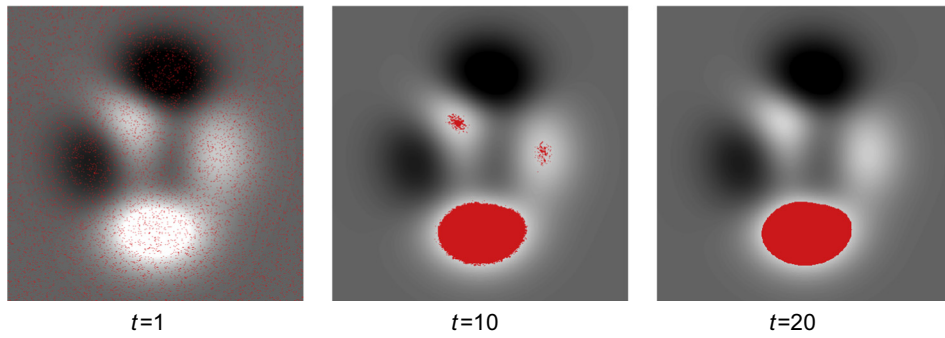
3.3.1.1. Performance on local and global optimums. A suitability layer with a polycentric distribution was generated in Matlab using the 'peak' function. Fig. 4 (a) shows that the suitability map contains a large area of the highest value in the bottom, which is designed to have enough area for urban-land allocation; two small areas of the highest suitability near the center, and two small areas of the lowest suitability adjacent to the left and top parts. The experiment examines whether the proposed model can generate such a pattern after sufficient iterations. The distribution can help to examine if the proposed model will be trapped at a local optimum. Fig. 4(b) shows that some ants located within the areas of less

high suitability values in several early iterations, but the pattern evolves quickly and almost all ants congregated at the bottom after 10 iterations. The pattern eventually stabilizes after 20 iterations, which indicates that the ACO can avoid the local optimum and obtain the best global solution.

3.3.1.2. Ability to obtain connected landscape patterns. If only compactness is considered, then the optimal pattern can reach maximum value when regular patches are generated even though they are isolated from each other. The ACO devised in this study considers both compactness and local connectivity for practical planning demand. In this test, small urban patches with different sizes but the same values of suitability are randomly scattered in the space, different size of searching



(a) Polycentric test data (suitability map)



(b) Optimization results at different iteration

Fig. 4. (a) Hypothetical data with polycentric distribution and (b) optimization results.

neighborhood window was designed to examine if the ACO can generate a connected and compact pattern. Fig. 5 lists the optimization results retrieved with different size of searching window.

Fig. 5 indicates that the searching window determines the size of the connected patch. The larger the searching window is, the bigger the connected patch is. Several big regular patches connected from all small patches are generated when the maximum searching window is set as 30 (Fig. 5b). All small patches are integrated into one patch when the maximum searching window is set as 60 (Fig. 5c). The whole optimization process proves that the ACO model can obtain the expected connected pattern by adjusting the searching window.

3.3.1.3. Efficiency in optimizing complex spatial structure. Another hypothetical data is prepared by using a suitability map of complex spatial structure. Fig. 6 shows the central areas of the highest suitability denoted by a question mark. If only suitability is considered for the optimal objective, then the expected pattern will be close to the original question mark. When more optimal objectives are demanded, the different

optimized patterns are expected. The experiment tests if the model can achieve the expected spatial pattern conforming to the designed multi-objectives. Varying weights are set for suitability and compactness, which represent the different preference for the optimal objectives.

Optimization results show if the higher weight is given for the suitability, then ACO can generate a pattern more similar with that of the highest suitability (Fig. 6a). Cells selected by artificial ants aggregate within the top parts provided that the two weights are given as the same values, and this area presents a big compact patch (Fig. 6b). The higher weight is given for the compactness, the more compact and regular pattern will be formed on the top parts of the highest suitability (Fig. 6c). The results illustrate that ACO can efficiently obtain expected patterns adaptive to the changed preference for different objectives.

3.3.2. Practicability of optimal UGBs retrieved by ACO

The results retrieved under different weight combinations can provide references for decision-making. According to the planning

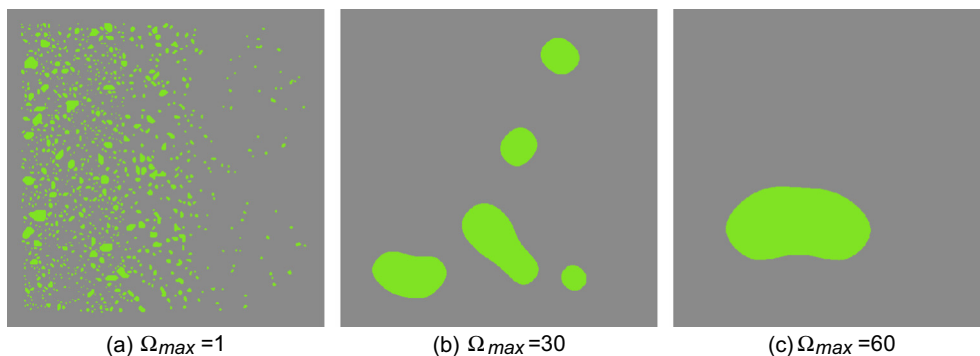


Fig. 5. Optimization results using a dynamic searching window.

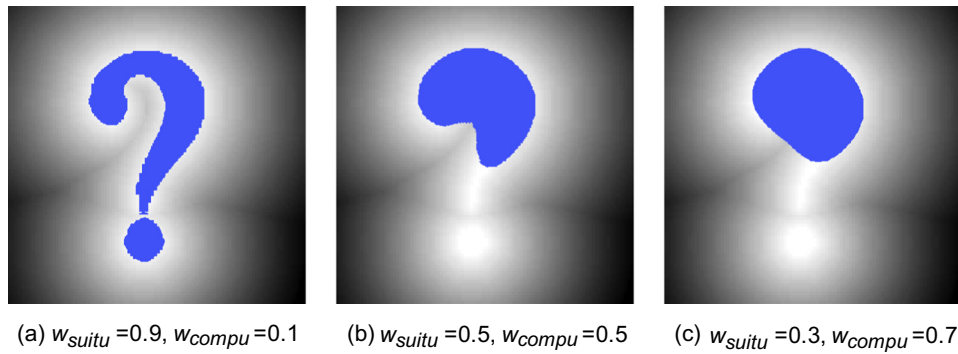


Fig. 6. Optimization results with different weights for objectives using hypothetical data.

demands of the case study area and sensitivity analysis of weight combinations, the relative weights of 6:1:3 for urban suitability, farmland preservation, and landscape compactness were eventually chosen by the planning preference to yield the optimized urban-land allocation pattern. Fig. 7(a) shows the final UGBs which was delimited by using ACO.

The potential growth pattern in a future year during the planning period can be used to assess the practicability of the UGBs. If most of the urban areas is contained within the delineated UGBs and pell-mell expansion is effectively controlled, then the UGBs are reasonable. The UGBs and remote sensing image are first compared visually. Fig. 7(a) shows the delineated UGBs and the present urban pattern overlaid on remote sensing image collected in 2015. The dark red areas represent urbanized regions (2005). The red arrows reflect the main directions of future urban expansion. The UGBs include almost all newly increased urban areas from 2005 to 2015. Three urban centers in Changsha, Xiangtan, and Zhuzhou distributed along the Xiangjiang River and a series of small urban clusters are exhibited in the optimization result. The

optimal pattern conforms to the polycentric development theory of urban agglomeration, which is feasible to make planning of smart urban growth.

Planning scenario designed by experts were further used to validate the practicability of optimal UGBs. Fig. 7(b) shows the planning map designed for CZTUA in current urban planning. Spatial conformity of urban areas among the three cities are expected by government. It is found that there is great spatial conformity of urban areas between the optimal UGBs and the planning scenario, and enough lands are reserved for urban growth in important regions. Moreover, quantitative comparison was also carried out between the model's outputs and planning scenario in terms of the three designed objectives in this study. The average utility of the three objectives was calculated, respectively, and the results were listed in Table 2. As for the utility of single objective, higher utilities of urban suitability and farmland preservation can be achieved from the optimal UGBs, while the utility of the landscape compactness is slightly lower than that of the planning scenario. The total utility of optimal UGBs is also higher than that of planning scenario, and the

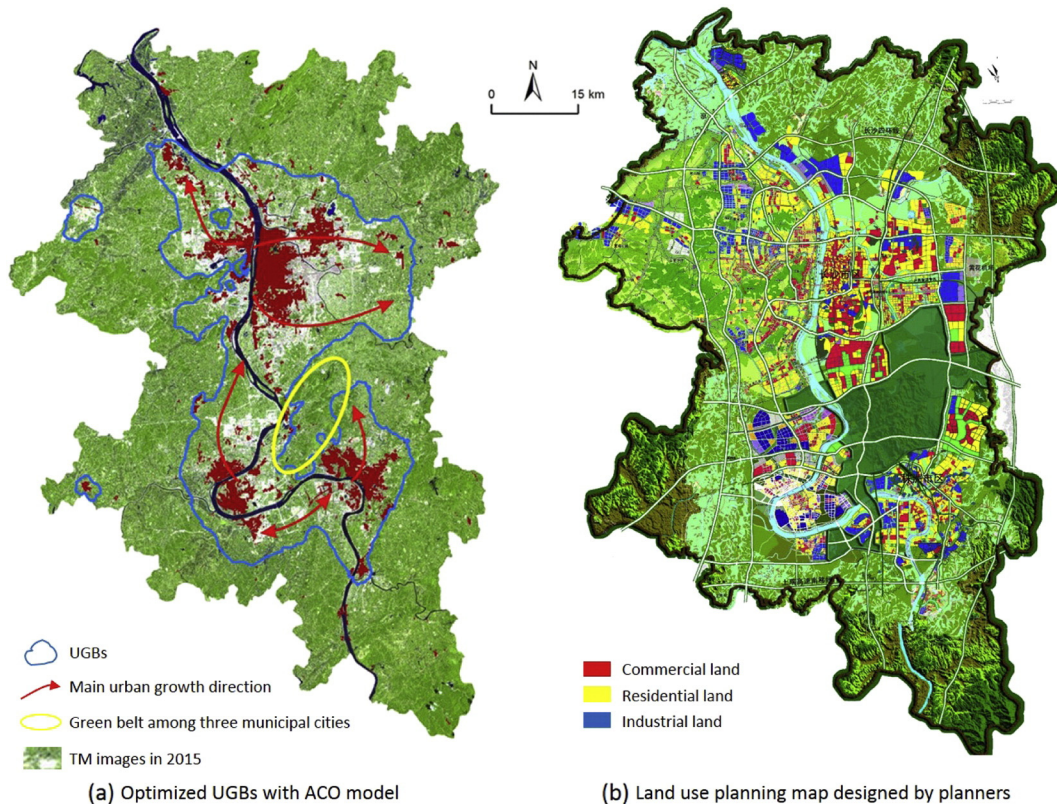


Fig. 7. Validation of the optimal UGBs with remote sensing image and the land use planning scenario.

Table 2
Comparison between optimal UGBs derived from ACO and planning scenario.

| Scenarios | f_{suitu} | f_{farmp} | f_{compu} | $F_{UGB}(w_{suitu}=0.6, w_{farmp}=0.3, w_{compu}=0.1)$ |
|-------------------|-------------|-------------|-------------|--|
| Optimal UGBs | 0.9548 | 0.6804 | 0.8972 | 0.8667 |
| Planning scenario | 0.9336 | 0.6432 | 0.9871 | 0.8518 |

values are at close quarters. Thus, the optimal UGBs derived from the ACO model can provide feasible reference for decision-making.

4. Conclusion

Quantitative delimitation of UGBs is a complex decision problem under given planning demands and constraints. This study developed an ACO-based framework with the integration of intrinsic urban processes and external planning interventions, which aims to generate a UGBs pattern that maximizes the utility value in terms of urban suitability, connected compactness, and farmland preservation. The main modifications include: (1) defining spatial objectives and constraints according to urban growth demands; (2) incorporating local connectivity into the suitability and compactness to delimit UGBs; and (3) updating the ants' status under the given rules and quantity constraint for each subregion to keep the structure balance.

The experiments using hypothetical data demonstrate that the ACO-based model will not be trapped at the local optima, can generate a connected pattern and optimize complex landscape pattern. The proposed model was tested in the core area of Changsha-Zhuzhou-Xiangtan urban agglomeration for the planning period 2006–2030 indicate that optimal urban-land allocation patterns can be efficiently derived from the modified ACO. The optimal UGBs delimited from the result of urban-land allocation is theoretically available and can well reflect main growth directions of Changsha-Zhuzhou-Xiangtan urban agglomeration.

This study suggests that the optimization-based model can well handle the trade-off between intrinsic urban processes and external planning interventions. The model validation shows that optimal UGBs can be generated by using the spatial optimization model under the given planning objectives and constraints. Our study has indicated that spatial optimization methods are attractive and plausible for delimiting UGBs in the fast growing areas.

References

Abbott, C., & Margheim, J. (2008). Imagining Portland's urban growth boundary: Planning regulation as cultural icon. *Journal of the American Planning Association*, 74(2), 196–208.

Akıncı, H., Özalp, A. Y., & Turgut, B. (2013). Agricultural land use suitability analysis using GIS and AHP technique. *Computers and Electronics in Agriculture*, 97, 71–82.

Altieri, L., Cocchi, D., Pezzi, G., Scott, E. M., & Ventrucci, M. (2014). Urban sprawl scatterplots for urban morphological zones data. *Ecological Indicators*, 36, 315–323.

Batty, M., & Xie, Y. C. (1999). Self-organized criticality and urban development. *Discrete Dynamics in Nature and Society*, 3(2–3), 109–124.

Bhatta, B. (2009). Modelling of urban growth boundary using geoinformatics. *International Journal of Digital Earth*, 2(4), 359–381.

Brookes, C. J. (2001). A genetic algorithm for designing optimal patch configuration in GIS. *International Journal of Geographical Information Science*, 15(6), 539–559.

Cao, K., Huang, B., Wang, S., & Lin, H. (2012). Sustainable land use optimization using boundary-based fast genetic algorithm. *Computers, Environment and Urban Systems*, 36(3), 257–269.

Cerreta, M., & De Toro, P. (2012). Urbanization suitability maps: A dynamic spatial decision support system for sustainable land use. *Earth System Dynamics*, 3(2), 157–171.

Cho, S., Chen, Z., Yen, S. T., & Eastwood, D. B. (2006). Estimating effects of urban growth boundary on land development. *Journal of Agricultural and Applied Economics*, 38(2), 287–298.

Dorigo, M., Maniezzo, V., & Colnari, A. (1996). The ant system: Optimization by a colony of cooperating agents. *IEEE Transactions on Systems Man and Cybernetics Part A-Systems and Humans*, 26(1), 1–13.

Gennaio, M., Hersperger, A. M., & Bürgi, M. (2009). Containing urban sprawl—Evaluating effectiveness of urban growth boundaries set by the Swiss Land Use Plan. *Land Use Policy*, 26(2), 224–232.

Godfray, H. C. J., Beddington, J. R., Crute, I. R., Haddad, L., Lawrence, D., Muir, J. F., ... Toulmin, C. (2010). Food security: The challenge of feeding 9 billion people. *Science*, 327, 812–818.

Gordon, A., Simondson, D., White, M., Moilanen, A., & Bekesy, S. A. (2009). Integrating conservation planning and land use planning in urban landscapes. *Landscape and Urban Planning*, 91(4), 183–194.

He, C. Y., Okada, N., Zhang, Q. F., Shi, P. J., & Zhang, J. S. (2006). Modeling urban expansion scenarios by coupling cellular automata model and system dynamic model in Beijing, China. *Applied Geography*, 26(3), 323–345.

Hepinstall, C. J., Coe, S., & Hutrya, L. R. (2013). Urban growth patterns and growth management boundaries in the Central Puget Sound, Washington, 1986–2007. *Urban Ecosystems*, 16(1), 109–129.

Hoekstra, A. Y., & Wiedmann, T. O. (2014). Humanity's unsustainable environmental footprint. *Science*, 344, 1114–1117.

Huang, B., Fery, P., Xue, L., & Wang, Y. (2008). Seeking the Pareto front for multi-objective spatial optimization problems. *International Journal of Geographical Information Science*, 22(5), 507–526.

Jun, M. J. (2004). The effects of Portland's urban growth boundary on urban development patterns and commuting. *Urban Studies*, 41(7), 1333–1348.

Kiran, G. S., & Joshi, U. B. (2013). Estimation of variables explaining urbanization concomitant with land-use change: A spatial approach. *International Journal of Remote Sensing*, 34(3), 824–847.

Knaap, G. J., & Hopkins, L. D. (2001). The inventory approach to urban growth boundaries. *Journal of the American Planning Association*, 67(3), 314–326.

Lambin, E. F., & Meyfroidt, P. (2011). Global land use change, economic globalization, and the looming land scarcity. *Proceedings of the National Academy of Sciences*, 108(9), 3465–3472.

Li, X. (2011). Emergence of bottom-up models as a tool for landscape simulation and planning. *Landscape and Urban Planning*, 100(4), 393–395.

Li, X., Chen, Y. M., Liu, X. P., Li, D., & He, J. Q. (2010). Concepts, methodologies, and tools of an integrated geographical simulation and optimization system. *International Journal of Geographical Information Science*, 25(4), 633–655.

Li, X., Lao, C. H., Liu, X. P., & Chen, Y. M. (2011). Coupling urban cellular automata with ant colony optimization for zoning protected natural areas under a changing landscape. *International Journal of Geographical Information Science*, 25(4), 575–593.

Ligmann-Zielinska, A., Church, R., & Jankowski, P. (2008). Spatial optimization as a generative technique for sustainable multi-objective land-use allocation. *International Journal of Geographical Information Science*, 22(6), 601–622.

Liu, Y. L., Wang, H., Ji, Y. L., Liu, Z. Q., & Zhao, X. (2012a). Land use zoning at the county level based on a multi-objective particle swarm optimization algorithm. *International Journal Environmental Research Public Health*, 9, 2801–2826.

Liu, X. P., Li, X., Shi, X., Huang, K. N., & Liu, Y. L. (2012b). A multi-type ant colony optimization (MACO) method for optimal land use allocation in large areas. *International Journal of Geographical Information Science*, 26(7), 1325–1343.

Long, Y., Gu, Y., & Han, H. (2012). Spatiotemporal heterogeneity of urban planning implementation effectiveness: Evidence from five urban master plans of Beijing. *Landscape and Urban Planning*, 108(2), 103–111.

Long, Y., Han, H., Lai, S., & Mao, Q. (2013). Urban growth boundaries of the Beijing metropolitan area: Comparison of simulation and artwork. *Cities*, 31, 337–348.

Masoomi, Z., Mesgari, M. S., & Hamrah, M. (2013). Allocation of urban land uses by multi-objective particle swarm optimization algorithm. *International Journal of Geographical Information Science*, 27(3), 542–566.

Mitsova, D., Shuster, W., & Wang, X. (2011). A cellular automata model of land cover change to integrate urban growth with open space conservation. *Landscape and Urban Planning*, 99(2), 141–153.

Nelson, A. C., & Moore, T. (1993). Assessing urban growth management: The case of Portland, Oregon, the USA's largest urban growth boundary. *Land Use Policy*, 10(4), 293–302.

Reza, M. I. H., & Abdullah, S. A. (2011). Regional index of ecological integrity: A need for sustainable management of natural resources. *Ecological Indicators*, 11(2), 220–229.

Santé, I., Crecente, R., & Miranda, D. (2008a). GIS-based planning support system for rural land-use allocation. *Computers and Electronics in Agriculture*, 63(2), 257–273.

Santé, I., Boullón, M., Crecente, R., & Miranda, D. (2008b). Algorithm based on simulated annealing for land-use allocation. *Computers & Geosciences*, 34(3), 259–268.

Santé, I., García, A. M., Miranda, D., & Crecente, R. (2010). Cellular automata models for the simulation of real-world urban processes: A review and analysis. *Landscape and Urban Planning*, 96(2), 108–122.

Tayyebi, A., Perry, P. C., & Tayyebi, A. H. (2014). Predicting the expansion of an urban boundary using spatial logistic regression and hybrid raster-vector routines with remote sensing and GIS. *International Journal of Geographical Information Science*, 28(4), 639–659.

Tayyebi, A., Pijanowski, B. C., & Tayyebi, A. H. (2011). An urban growth boundary model using neural networks, GIS and radial parameterization: An application to Tehran, Iran. *Landscape and Urban Planning*, 100(1), 35–44.

Tudes, S., & Yigiter, N. D. (2010). Preparation of land use planning model using GIS based on AHP: Case study Adana-Turkey. *Bulletin of Engineering Geology and the Environment*, 69(2), 235–245.

Venkataraman, M. (2014). Analysing urban growth boundary effects on the City of Bengaluru. *Economic and Political Weekly*, 49(48), 54–61.

Washington-Ottobro, C., Pijanowski, B., Campbell, D., Olson, J., Maitima, J., Musili, A., ... Mwangi, A. (2010). Using a role-playing game to inform the development of land-use models for the study of a complex socio-ecological system. *Agricultural Systems*, 103(3), 117–126.

Wei, Y. D., & Ye, X. (2014). Urbanization, urban land expansion and environmental change in China. *Stochastic Environmental Research and Risk Assessment*, 28(4), 757–765.

Zheng, X. Q., & Lv, L. N. (2016). A WOE method for urban growth boundary delineation and its applications to land use planning. *International Journal of Geographical Information Science*, 30(4), 691–707.